A Novel Power Injection Model of IPFC for Power Flow Analysis Inclusive of Practical Constraints

Yankui Zhang, Yan Zhang, and Chen Chen, *Senior Member, IEEE*

***Abstract*—This paper describes a novel power injection model (PIM) of interline power flow controller (IPFC) for power flow analysis. In this model, the impedance of the series coupling transformer and the line charging susceptance are all included. In this situation, it is proved that the original structure and symmetry of the admittance matrix can still be kept, and thus, the Jacobian matrix can keep the block-diagonal properties, and sparsity technique can be applied. The IPFC state variables are adjusted simultaneously with the network state variables in order to achieve the specified control targets. Furthermore, the model can take into account the practical constraints of IPFC in Newton power flow. Numerical results based on the IEEE 57-bus and IEEE 300-bus systems are used to demonstrate the effectiveness and performance of the IPFC model.**

***Index Terms*—Interline power flow controller (IPFC), Newton power flow, power injection model (PIM), practical constraints of IPFC, voltage source model (VSM).**

I. Introduction

THE LAST generation FACTS controllers using the self-commutated voltage sourced converter (VSC) usually include the static synchronous compensator (STATCOM), static synchronous series compensator (SSSC), unified power flow controller (UPFC), and interline power flow controller (IPFC) [1]–[7]. The STATCOM is usually employed as shunt reactive compensator and SSSC as series active or reactive compensator. The UPFC concept provides a powerful tool for the cost-effective utilization of individual transmission lines by facilitating the independent control of both active and reactive power flow, and thus the maximization of real power transfer at minimum losses, in the line. However, the UPFC and SSSC can control power flow of only one transmission line. Compared with the UPFC and SSSC, the IPFC has much more flexible topologies, consists of at least two converters, and can be used to control power flows of a group of lines. It can be anticipated that the IPFC may be used to solve the complex transmission network congestion management problems that transmission companies are now facing in the transmission open-access environment. This is the case of the convertible static compensator (CSC) installed at the Marcy Substation of the New York Power Authority (NYPA) as party of project that will increase power transfer capability and maximize the use of the existing transmission network [8], [9].

Manuscript received March 30, 2005; revised August 15, 2005. Paper no. TPWRS-00176-2005.

The authors are with the Department of Electrical Engineering, Shanghai Jiao Tong University, Shanghai, China (e-mail: zhangyankui@sjtu.edu.cn; zhang_yan@sjtu.edu.cn; chchen@online.sh.cn).

Digital Object Identifier 10.1109/TPWRS.2006.882458

Power flow calculations are performed frequently in power system operation, planning, and control. With the practical applications of the VSC-based FACTS in power systems, computer modeling of these is also of great concern. So far, much effort has been paid in the modeling of the UPFC for power flow and optimal power flow [10]–[17], while few publications [18], [19] can be found in the modeling of the IPFC, especially inclusive of the practical constraints. This motivates the author to develop a new model for IPFC in power flow analysis.

Researchers have made progress on the VSC-based FACTS devices modeling aspects. The existing steady-state models can mainly be classified into two categories: One is a decoupled model [10], [11], and the other is a coupled model. In a decoupled model, the FACTS devices are usually replaced with a fictitious PQ or PV bus, which results in the modification of Jacobian matrix structure. A coupled model generally consists of two major models: voltage source model (VSM) [12], [13], [18]–[20] and power injection model (PIM) [14]–[17]. In VSM, the converters are formulated as voltage injections, where the control parameters are directly treated as state variables. The VSM has a good convergence property, and the converter variables from power flow can be used to directly initialize dynamic simulation programs. However, it destroys the symmetric characteristics of the admittance matrix [16]. Derived from the VSM, the PIM with the conversion of inserted voltage source to power injections to the related buses is allowed to keep the symmetry of the admittance matrix. In the PIM of [14] and [15], the control parameters of converters are also treated as state variables. Reference [16] presents another type of PIM, in which the active and reactive power injections are directly considered as independent state variables. However, the control parameters can only be calculated after the solution of the power flow equation, and this method may have poor convergence property [19]. It must be pointed out that two PIMs above do not consider the line charging susceptance. In addition, how to handle the practical constraints of FACTS devices is an important problem [21], [22]. It was not reported in the publications how the constraints of IPFC are handled in their power flow programs.

This paper describes a novel power injection model of IPFC for power flow analysis. In this model, the impedance of the series converter transformer and the line charging susceptance are all included. In this situation, it is proved that the original structure and symmetry of the admittance matrix can still be kept, and thus, the Jacobian matrix can keep the block-diagonal properties, and sparsity technique can be applied. The IPFC state variables are adjusted simultaneously with the network state variables in order to achieve the specified control targets Furthermore, the model can take into account the practical constraints of IPFC, and the detailed implementation of these in Newton power flow is presented.

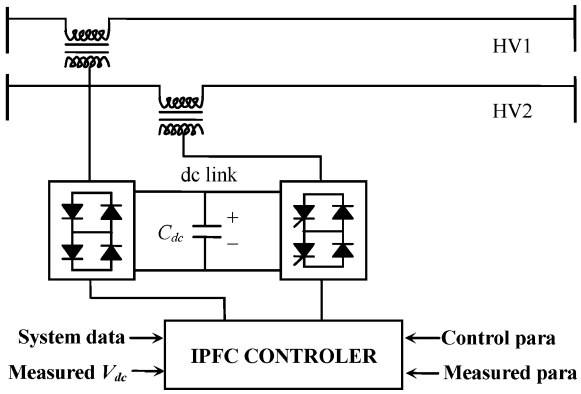

Fig. 1. Schematic diagram of two-converter IPFC.

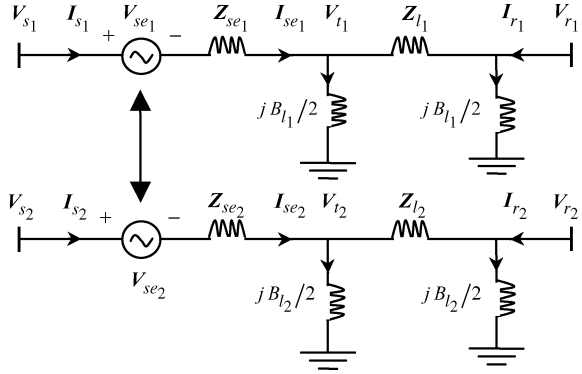

Fig. 2. Equivalent circuit of two-converter IPFC using voltage source.

II. Power Injection Model of IPFC

A. Operation Principles of IPFC

In its general form, the IPFC employs a number of dc to ac converters, each providing series compensation for a different line. The converters are linked together at their dc terminals and connected to the ac systems through their series coupling transformers [7]. With this scheme, in addition to providing series reactive compensation, any converter can be controlled to supply active power to the common dc link from its own transmission line. For an IPFC with m series converters, the control degree of freedom of $m-1$ series converters is two, except that one series converter has one control degree of freedom since the active power exchange among the m series converters should be balanced at any time [18]. For the sake of simplicity, the IPFC with two series converters shown in Fig. 1 is used to show the basic operation principles. The mathematical derivation is applicable to an IPFC with any number of series converters.

B. Equivalent Circuit and Power Injections of IPFC

Fig. 2 shows the equivalent circuit of an IPFC with two series converters. In this circuit, $\boldsymbol{V}_{se_n} = V_{se_n}\angle\theta_{se_n}$ is the complex controllable series injected voltage. $\boldsymbol{Z}_{se_n} = R_{se_n} + jX_{se_n}$ is the series transformer impedance. $\boldsymbol{V}_{s_n} = V_{s_n}\angle\theta_{s_n}$ and $\boldsymbol{V}_{r_n} = V_{s_n}\angle\theta_{r_n}$ are, respectively, the complex bus voltages at buses s_n and r_n. $\boldsymbol{Z}_{l_n} = R_{l_n} + jX_{l_n}$ and B_{l_n} represent the line series impedance and line charging susceptance, respectively, while n is the line number ($n = 1,2\ldots.$). From Fig. 2, for one of the lines, the relations can be derived as follows:

$$\boldsymbol{V}_{s_n} = \boldsymbol{V}_{se_n} + \boldsymbol{I}_{s_n}\boldsymbol{Z}_{se_n} + \boldsymbol{V}_{t_n} \tag{1}$$

$$\boldsymbol{I}_{s_n} = \frac{(\boldsymbol{V}_{t_n} - \boldsymbol{V}_{r_n})}{\boldsymbol{Z}_{l_n}} + \boldsymbol{j}\frac{\boldsymbol{B}_{l_n}}{2}\boldsymbol{V}_{t_n}. \tag{2}$$

We can express $\boldsymbol{V}_{t_n}$ and $\boldsymbol{I}_{s_n}$ according to $\boldsymbol{V}_{r_n}$ and $\boldsymbol{I}_{r_n}$ as

$$\boldsymbol{V}_{t_n} = \left(1 + \boldsymbol{j}\frac{\boldsymbol{B}_{l_n}}{2}\boldsymbol{Z}_{l_n}\right)\boldsymbol{V}_{r_n} - \boldsymbol{I}_{r_n}\boldsymbol{Z}_{l_n} \tag{3}$$

$$\boldsymbol{I}_{s_n} = \left(\boldsymbol{j}\boldsymbol{B}_{l_n} - \frac{\boldsymbol{B}_{l_n}^2}{4}\boldsymbol{Z}_{l_n}\right)\boldsymbol{V}_{r_n} - \left(1 + \boldsymbol{j}\frac{\boldsymbol{B}_{l_n}}{2}\boldsymbol{Z}_{l_n}\right)\boldsymbol{I}_{r_n}. \tag{4}$$

From (1)–(4), we can express $\boldsymbol{I}_{s_n}$ and $\boldsymbol{I}_{r_n}$ in terms of $\boldsymbol{V}_{s_n}$, $\boldsymbol{V}_{r_n}$, and $\boldsymbol{V}_{se_n}$ as

$$\boldsymbol{I}_{s_n} = \left(\boldsymbol{D} - \frac{\boldsymbol{M}\boldsymbol{E}}{\boldsymbol{N}}\right)\boldsymbol{V}_{r_n} + \frac{\boldsymbol{E}}{\boldsymbol{N}}\boldsymbol{V}_{s_n} - \frac{\boldsymbol{E}}{\boldsymbol{N}}\boldsymbol{V}_{se_n} \tag{5}$$

$$\boldsymbol{I}_{r_n} = \frac{\boldsymbol{M}}{\boldsymbol{N}}\boldsymbol{V}_{r_n} - \frac{1}{\boldsymbol{N}}\boldsymbol{V}_{s_n} + \frac{1}{\boldsymbol{N}}\boldsymbol{V}_{se_n} \tag{6}$$

where

$$\boldsymbol{D} = \left(\boldsymbol{j}\boldsymbol{B}_{l_n} - \boldsymbol{Z}_{l_n}\boldsymbol{B}_{l_n}^2/4\right),\ \boldsymbol{E} = \left(1 + \boldsymbol{j}\boldsymbol{Z}_{l_n}\boldsymbol{B}_{l_n}/2\right)$$
$$\boldsymbol{M} = \boldsymbol{Z}_{se_n}\boldsymbol{D} + \boldsymbol{E}, \boldsymbol{N} = \boldsymbol{Z}_{se_n}\boldsymbol{E} + \boldsymbol{Z}_{l_n}.$$

Equations (5) and (6) can also be written in matrix form as

$$\begin{bmatrix}\boldsymbol{I}_{s_n}\\ \boldsymbol{I}_{r_n}\end{bmatrix} = \begin{bmatrix}\boldsymbol{A}_{ss_n} & \boldsymbol{A}_{sr_n}\\ \boldsymbol{A}_{rs_n} & \boldsymbol{A}_{rr_n}\end{bmatrix}\begin{bmatrix}\boldsymbol{V}_{s_n}\\ \boldsymbol{V}_{r_n}\end{bmatrix} + \begin{bmatrix}\boldsymbol{W}_{ss_n}\\ \boldsymbol{W}_{rs_n}\end{bmatrix}\boldsymbol{V}_{se_n} \tag{7}$$

where

$$\boldsymbol{A}_{ss_n} = \frac{\boldsymbol{E}}{\boldsymbol{N}},\ \boldsymbol{A}_{rr_n} = \frac{\boldsymbol{M}}{\boldsymbol{N}},\ \boldsymbol{A}_{sr_n} = \boldsymbol{D} - \frac{\boldsymbol{M}\boldsymbol{E}}{\boldsymbol{N}}$$
$$\boldsymbol{A}_{rs_n} = -\frac{1}{\boldsymbol{N}},\ \boldsymbol{W}_{ss_n} = -\frac{\boldsymbol{E}}{\boldsymbol{N}},\ \boldsymbol{W}_{rs_n} = \frac{1}{\boldsymbol{N}}.$$

We can prove that the matrix $\boldsymbol{A}$ is symmetrical, i.e.,

$$\boldsymbol{A}_{sr_n} = \boldsymbol{A}_{rs_n}. \tag{8}$$

The symmetry of matrix $\boldsymbol{A}$ is very important, which can make $\boldsymbol{A}_{ss_n}$ and $\boldsymbol{A}_{rr_n}$ be divided into two parts as

$$\boldsymbol{A}_{ss_n} = -\boldsymbol{A}_{sr_n} + \boldsymbol{A}_{s_n}^0,\ \boldsymbol{A}_{s_n}^0 = \boldsymbol{D} + \frac{\boldsymbol{E}(1+\boldsymbol{M})}{\boldsymbol{N}}$$
$$\boldsymbol{A}_{rr_n} = -\boldsymbol{A}_{rs_n} + \boldsymbol{A}_{r_n}^0,\ \boldsymbol{A}_{r_n}^0 = \frac{(\boldsymbol{M}-1)}{\boldsymbol{N}}. \tag{9}$$

Equation (7) can also be expressed by the equivalent circuit shown in Fig. 3.

From Fig. 3, the active and reactive power injections at buses s_n and r_n associated with two current sources can be easily calculated as follows (for the sake of simplicity, the resistances

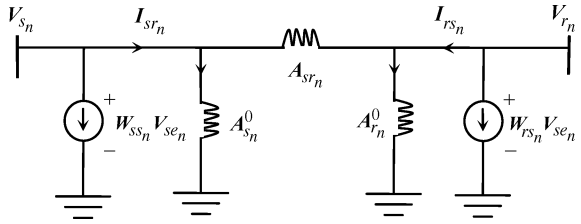

Fig. 3. Representation of IPFC using current source.

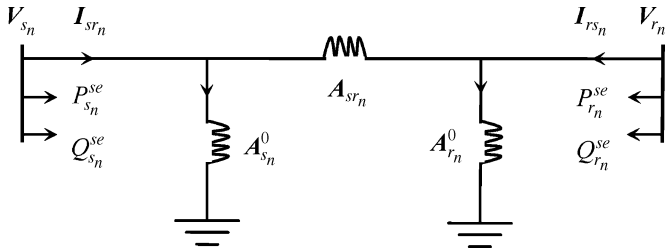

Fig. 4. Power injections π-model of IPFC.

of the transmission lines and the series coupling transformers are neglected):

$$P^{se}_{s_n} = \mathrm{Re}\left\{\boldsymbol{V}_{s_n}(\boldsymbol{W}_{ss_n}\boldsymbol{V}_{se_n})^*\right\} = \frac{\left(1-\frac{B_{l_n}}{2}X_{l_n}\right)}{H}V_{s_n}V_{se_n}\sin(\theta_{s_n}-\theta_{se_n}) \quad (10)$$

$$Q^{se}_{s_n} = \mathrm{Im}\left\{\boldsymbol{V}_{s_n}(\boldsymbol{W}_{ss_n}\boldsymbol{V}_{se_n})^*\right\} = \frac{-\left(1-\frac{B_{l_n}}{2}X_{l_n}\right)}{H}V_{s_n}V_{se_n}\cos(\theta_{s_n}-\theta_{se_n}) \quad (11)$$

$$P^{se}_{r_n} = \mathrm{Re}\left\{\boldsymbol{V}_{r_n}(\boldsymbol{W}_{rs_n}\boldsymbol{V}_{se_n})^*\right\} = \frac{-V_{r_n}V_{se_n}}{H}\sin(\theta_{r_n}-\theta_{se_n}) \quad (12)$$

$$Q^{se}_{r_n} = \mathrm{Im}\left\{\boldsymbol{V}_{r_n}(\boldsymbol{W}_{rs_n}\boldsymbol{V}_{se_n})^*\right\} = \frac{V_{r_n}V_{se_n}}{H}\cos(\theta_{r_n}-\theta_{se_n}) \quad (13)$$

where $H = X_{se_n}(1-(B_{l_n}/2)X_{l_n})+X_{l_n}$.

The equivalent power injection model of an IPFC is shown in Fig. 4. It can be concluded that the admittance matrix still keeps the same structure and symmetry as that of the case without IPFC.

The currents from buses s_n and r_n can be, respectively, expressed as

$$\boldsymbol{I}_{sr_n} = (\boldsymbol{V}_{s_n}-\boldsymbol{V}_{r_n})\boldsymbol{A}_{sr_n}+\boldsymbol{V}_{s_n}\boldsymbol{A}^0_{s_n} \quad (14)$$

$$\boldsymbol{I}_{rs_n} = (\boldsymbol{V}_{r_n}-\boldsymbol{V}_{s_n})\boldsymbol{A}_{sr_n}+\boldsymbol{V}_{r_n}\boldsymbol{A}^0_{r_n}. \quad (15)$$

The active and reactive powers from buses s_n and r_n can be, respectively, expressed as

$$P_{sr_n} = \mathrm{Re}\left(\boldsymbol{V}_{s_n}\boldsymbol{I}^*_{sr_n}\right) = \frac{-1}{H}V_{s_n}V_{r_n}\sin\theta_{sr_n} \quad (16)$$

$$Q_{sr_n} = \mathrm{Im}\left(\boldsymbol{V}_{s_n}\boldsymbol{I}^*_{sr_n}\right) = \frac{-\left(1+\frac{B_{l_n}X_{l_n}}{2}\right)V^2_{s_n}+V_{s_n}V_{r_n}\cos\theta_{sr_n}}{H} \quad (17)$$

$$P_{rs_n} = \mathrm{Re}\left(\boldsymbol{V}_{r_n}\boldsymbol{I}^*_{rs_n}\right) = \frac{-1}{H}V_{s_n}V_{r_n}\sin\theta_{rs_n} \quad (18)$$

$$Q_{rs_n} = \mathrm{Im}\left(\boldsymbol{V}_{r_n}\boldsymbol{I}^*_{rs_n}\right) = \frac{V_{r_n}}{H}\left(-V_{r_n}+V_{s_n}\cos\theta_{rs_n} - V_{r_n}\left(X_{se_n}\left(B_{l_n}-\frac{B^2_{l_n}X_{l_n}}{4}\right)+\frac{B_{l_n}X_{l_n}}{2}\right)\right). \quad (19)$$

As IPFC neither absorbs nor injects active power with respect to the ac system, the active power exchange between or among the converters via the dc link is zero, i.e.,

$$P_{dc} = \sum_n P_{ex_n} = 0 \quad (20)$$

where

$$P_{ex_n} = \mathrm{Re}\left(\boldsymbol{V}_{se_n}\boldsymbol{I}^*_{s_n}\right) = \left(B_{l_n}-\frac{B^2_{l_n}X_{l_n}}{4}+\frac{G}{H}\right)V_{se_n}V_{r_n}\sin(\theta_{se_n}-\theta_{r_n}) - \frac{\left(1-\frac{B_{l_n}}{2}X_{l_n}\right)V_{s_n}V_{se_n}\sin(\theta_{se_n}-\theta_{s_n})}{H} = 0 \quad (21)$$

where $G = (-X_{se_n}(B_{l_n}-X_{l_n}(B^2_{l_n}/4))+1-X_{l_n}(B_{l_n}/2))(1-X_{l_n}(B_{l_n}/2))$.

C. Power Flow Controls of IPFC

The IPFC shown in Fig. 1 can control active and reactive power flows of the master line s_1-r_1 and active or reactive power flow of the slave line s_2-r_2. It is arbitrary to choose a line as the master or slave one according to the actual demand. For the slave line, it is assumed that the active power control is used while the reactive power flow control is released. Alternatively, the reactive power control can be used while the active power flow needs to be released. In principle, either scheme can be implemented in the Newton power flow.

The active and reactive power flow control constraints of two lines at the receiving buses are

$$P_{rs_n}-P^{sp}_{rs_n} = 0 \quad (22)$$

$$Q_{rs_n}-Q^{sp}_{rs_n} = 0 \quad (23)$$

where $P^{sp}_{rs_n}$ and $Q^{sp}_{rs_n}$ are, respectively, the specified active and reactive power flow setpoints of the lines s_n-r_n.

Though the paper only deals with the power flow control mode of IPFC, other modes such as the fixed voltage injection mode, etc. [7] also can be easily achieved in this framework. In the fixed voltage injection mode, the converter simply generates a fixed series voltage magnitude and phase angle. For the master line, the series voltage magnitude and angle are specified. For the slave line, either the series voltage magnitude or angle is specified. For example, when the series voltage magnitude is specified, the series voltage angle will be adjusted during

power flow solutions to meet the active power exchange determined by the master converter.

Equations (22) and (23) can be generally written as

$$\Delta \boldsymbol{C}(\boldsymbol{X}) = \boldsymbol{C}(\boldsymbol{X}) - \boldsymbol{C}^{sp} = 0 \tag{24}$$

where $\boldsymbol{X} = (V_{s_n}, \theta_{s_n}, V_{r_n}, \theta_{r_n}, V_{se_n}, \theta_{se_n})$.

D. IPFC Operating Constraints

The practical feasibility of steady-state and transient-state operating conditions of IPFC may be constrained by the ratings of the converter and by some operating limits. Three main constraints can be considered [20]–[22]:

1) $I_{se_n}^{\max}$: maximum series injected current;
2) $V_{se_n}^{\max}$: maximum series injected voltage;
3) $P_{ex_n}^{\max}$: maximum active power exchange on the dc link.

The maximum series injected voltage is the voltage rating of the series converter. The maximum series current is the current rating of the series converter at which level it can operate continuously. The maximum active power exchange via the dc link is strictly an equipment rating [17]. These practical limits imposed on IPFC together with the power system conditions define an achievable range of operating points. All these limits should be enforced in power flow calculations.

III. Implementation of IPFC Model in Newton Power Flow Algorithm

A. Newton Power Flow Algorithm

From Fig. 4, the PIM of IPFC can be easily incorporated into the existing Newton power flow program. The power balance equations can be expressed as

$$\Delta P_{s_n} = P_{s_n}^g - P_{s_n}^d - P_{s_n}^{se} - P_{s_n} = 0 \tag{25}$$
$$\Delta Q_{s_n} = Q_{s_n}^g - Q_{s_n}^d - Q_{s_n}^{se} - Q_{s_n} = 0 \tag{26}$$
$$\Delta P_{r_n} = P_{r_n}^g - P_{r_n}^d - P_{r_n}^{se} - P_{r_n} = 0 \tag{27}$$
$$\Delta Q_{r_n} = Q_{r_n}^g - Q_{r_n}^d - Q_{r_n}^{se} - Q_{r_n} = 0 \tag{28}$$

where P_k and Q_k are, respectively, the active and reactive power flows leaving bus k ($k = s_n, r_n \ldots$). These are the sum of the active and reactive power flows, including those given by (16)–(19), respectively. While P_k^g and Q_k^g are, respectively, the active and reactive power entering bus k, and P_k^d and Q_k^d are, respectively, the active and reactive load leaving bus k.

Equations (25)–(28) can be generally written as

$$\Delta \boldsymbol{F}(\boldsymbol{X}) = \boldsymbol{F}(\boldsymbol{X}) - \boldsymbol{F}^{sp} = 0. \tag{29}$$

Newton power flow algorithm with simultaneous solution of equations (20), (24), and (29) may be represented as

$$\left[\frac{\partial \boldsymbol{P}_{dc}(\boldsymbol{X})}{\partial \boldsymbol{X}} \;\; \frac{\partial \Delta \boldsymbol{C}(\boldsymbol{X})}{\partial \boldsymbol{X}} \;\; \frac{\partial \Delta \boldsymbol{F}(\boldsymbol{X})}{\partial \boldsymbol{X}}\right]^T [\Delta \boldsymbol{X}] = \begin{bmatrix} -\boldsymbol{P}_{dc} \\ -\Delta \boldsymbol{C}(\boldsymbol{X}) \\ -\Delta \boldsymbol{F}(\boldsymbol{X}) \end{bmatrix} \tag{30}$$

where the superscript T indicates transposition.

Because the IPFC model can keep the original structure and symmetry of the admittance matrix, the Jacobian matrix block associated with $\Delta \boldsymbol{F}(\boldsymbol{X})$ and the nodal network state variables has the same structure as that of the system Jacobian matrix of conventional power flow. In addition, the IPFC variables are adjusted simultaneously with the network variables in order to achieve the specified control targets. All these will lead to robust and efficient iterative solutions.

B. Enforcement of the Operation Constraints

1) Principle of the Constraint Enforcement: Finding all possible operating points of the system while respecting the operation constraints of IPFC is very difficult, especially the condition (20) introduces nonlinearity to the IPFC model and adds significant complexity to the problem. From this point of view, this paper only aims at the two-converter IPFC shown in Fig. 1, and the method described as follows provides only an alternative in handling the operation constraints of IPFC for power flow calculations.

2) Method of the Constraints Enforcement: Among the limit violations of IPFC, the series current limit violation is first eliminated, by which the new power flow setpoint can be established. For the master line, the specified reactive power flow is first reduced to zero. If reducing it to zero can eliminate the series current limit violation, the reactive power flow control is released; otherwise, the specified reactive power flow is maintained at zero, and the active power flow control is released. For the salve line, only the active or reactive power flow control is released. Meanwhile, the series current is kept at its limit as

$$I_{se_n} - I_{se_n}^{\max} = 0. \tag{31}$$

This method emphasizes the importance of the active power transfer and control. After the series current limit violation is eliminated, the limits on the series voltage and active power exchange may prevent IPFC from controlling power flow at the established setpoint subject to the series current limit. The two limits may result in three possible states as follows.

State 1: $V_{se_n}^{\max}$ is violated, while $P_{ex_n}^{\max}$ is a dependent variable. For the master line, if possible, the active power flow is maintained at the established value and reactive power flow control is released; otherwise, the reactive power flow is maintained at the established value, and active power flow control is released. For the salve line, only the active or reactive power flow control is released. Meanwhile, V_{se_n} is kept at its limit as

$$V_{se_n} - V_{se_n}^{\max} = 0. \tag{32}$$

State 2: $P_{ex_n}^{\max}$ is violated, while V_{se_n} is a dependent variable. In this case, for the master line, reactive power flow control is first released, and active power flow is maintained at its established value; for the salve line, only the active or reactive power flow control is released. Meanwhile, P_{ex_n} is kept at its limit as

$$P_{ex_n} - P_{ex_n}^{\max} = 0. \tag{33}$$

State 3: $V_{se_n}^{\max}$ and $P_{ex_n}^{\max}$ are both violated. In this case, two of the three power flow control equations are released, such as, for the master line, both the active and reactive power

flow control are released. Meanwhile, $V_{se_n}^{\max}$ and $P_{ex_n}^{\max}$ are enforced by (32) and (33).

3) Starting Criterion of the Constraints Enforcement: The starting criterion for checking the constraints of IPFC is the use of the active power exchange mismatch equation (20) [13]. At each iteration, this power mismatch equation provides an accurate indicator of the convergence process by which the activation of the constraints enforcement can be started. The enforcement is activated just after (20) is within a specified tolerance, such as 10^{-3}. If during two continuous iteration step, a particular constraint is continuously violated, the constraint is enforced while the original control objective is released.

It can be seen that the formulation of the Newton power flow with the constraints enforcement has exactly the same structure as that of the Newton power flow without it. This property makes the algorithm easy and efficient.

IV. Case Studies and Results

In this section, based on the IEEE 57-bus and IEEE 300-bus systems [23], numerical results are carried out to show the effectiveness and performance of the IPFC model. For all the cases, the convergence tolerance ε is 10^{-10}. The limits of IPFC are set to $V_{se_n}^{\max} = 1.0$, $I_{se_n}^{\max} = 10.0$, and $P_{ex_n}^{\max} = 1.0$ (p.u). System base MVA is 100. The initial values of the voltage magnitude and angle of an IPFC may be set to -100^0 and 0.2 p.u. It must be pointed out that, although the IPFC has two different sending buses shown in Fig. 1, the sending buses are the same bus in most cases.

A. Power Flow Convergence

Five cases are used to verify the convergence property of the IPFC model. We mainly focus on the impact of the small series transformer reactance and the line power setpoint.

Case 1) For the IEEE 57-bus system, an IPFC on the lines 38–44 (48) is operating at the base and high power flow setpoints, respectively, while the series transformer reactance is set to different values. The base flow setpoint is the power level without IPFC. The high flow setpoints are the much larger active power levels achieved by IPFC with sufficient reactive power to maintain appropriate voltage levels. The reactances for the two lines are 0.0585 and 0.0482 p.u.

Case 2) It is similar to case 1, except that an IPFC is inserted into the lines 231–237 (190) of the IEEE 300-bus system. The reactance for the two lines are 0.0006 and 0.0022 p.u.

Case 3) For the IEEE 57-bus system, an IPFC on the lines 15–13 (14) is operating with different power setpoints.

Case 4) For the IEEE 300-bus system, an IPFC on the lines 188–186 (187) is operating with different power setpoints.

Case 5) It is similar to case 4, except that three IPFCs are, respectively, inserted into the lines 2–6 (8), 42–16 (39), and 119–118 (120).

The IPFC power flow convergence results for cases 1–4 are, respectively, summarized in Tables I–IV.

TABLE I
IEEE 57-Bus System IPFC Power Flow Convergence for Case 1

X_{se_n} (p.u)	Number of iterations (base flow)	Number of iterations (high flow)
0.1	5	6
0.01	5	7
0.001	5	7
0.0001	5	8

TABLE II
IEEE 300-Bus System IPFC Power Flow Convergence for Case 2

X_{se_n} (p.u)	Number of iterations (base flow)	Number of iterations (high flow)
0.1	7	8
0.01	7	10
0.001	8	10
0.0001	9	10

TABLE III
IEEE 57-Bus System IPFC Power Flow Convergence for Case 3

P_{13-15}^{sp} (MW)	Q_{13-15}^{sp} (MVAr)	P_{14-15}^{sp} (MW)	Number of iterations
-49.0	8.5	-68.0	6 (base flow)
-79.0	-5.5	-38.0	5
49.0	-8.5	-117.0	8
-69.0	-2.5	-88.0	8

TABLE IV
IEEE 300-Bus System IPFC Power Flow Convergence for Case 4

$P_{186-188}^{sp}$ (MW)	$Q_{186-188}^{sp}$ (MVAr)	$P_{187-188}^{sp}$ (MW)	Number of iterations
714.0	123.0	485.0	8 (base flow)
614.0	103.0	285.0	7
814.0	153.0	385.0	8
514.0	83.0	685.0	6

From Tables I and II, it can be seen that the number of iterations is not sensitive to the size of the series transformer reactance, especially when the line reactance is larger. The reason may be that IPFC is embedded in the lines. From Tables III and IV, it is clear that the line power flow setpoints have a little effect on the convergence.

The IPFC model is implemented within the Visual C++ 6.0 environment, and the computation is performed on a computer with 1.4-GHz CPU and 256-MB random-access memory (RAM). For the IEEE 57-bus system, the computation time is less than 0.5 s for converged cases 1 and 3. For the IEEE 300-bus system, the computation time is less than 2 s for converged cases 2 and 4 and less than 4 s for case 5. The computation time may be affected by the programming skills.

B. IPFC Power Flow Control With and Without the Constraints Enforcement

Based on the IEEE 300-bus system, two cases are used to exhibit the power flow control capability of IPFC without the constraints enforcement.

Case 6) An IPFC on the lines 130–167(168) is operating with the setpoint $P_{167-130}^{sp} = -220$ MW,

TABLE V
IPFC POWER FLOW SOLUTIONS FOR CASES 6 AND 7

Case 6	Case 7
V_{130}= 1.007, V_{167} = 0.946 V_{168}=0.987	V_{130} = 1.01, V_{167} = 0.991 V_{168} =0.995
$P_{167-130}$ = -230.0, $Q_{167-130}$ = -10.0 $P_{168-130}$ = -200.0, $Q_{168-130}$ = -6.37	$P_{167-130}$ = -350.0, $Q_{167-130}$ = -80.0 $P_{168-130}$ = -350.0, $Q_{168-130}$ = 25.84
V_{se_1} = 0.2682, θ_{se_1} = -103.26^0 V_{se_2} = 0.2422, θ_{se_2} = -94.91^0	V_{se_1} = 0.1337, θ_{se_1} = -95.35^0 V_{se_2} = 0.1116, θ_{se_2} = -94.87^0
I_{se_1} = 2.337, I_{se_2} =2.030 (p.u)	I_{se_1} = 3.624, I_{se_2} =3.531 (p.u)
P_{ex_1}=1.113, P_{ex_2} = -1.113 (MW)	P_{ex_1} = -6.753, P_{ex_2} =6.753 (MW)

TABLE VI
IPFC POWER FLOW SOLUTIONS FOR CASES 8 AND 9

Case 8	Case 9
V_{130}= 1.007, V_{167} = 0.947 V_{168}=0.986	V_{130}= 1.009, V_{167} = 0.960 V_{168}=1.013
$P_{167-130}$ = -220.0, $Q_{167-130}$ = -12.0 $P_{168-130}$ = -204.5, $Q_{168-130}$ = 1.722	$P_{167-130}$ = -345.4, $Q_{167-130}$ = 0.00 $P_{168-130}$ = -350.0, $Q_{168-130}$ = -82.40
V_{se_1} = 0.2816, θ_{se_1} = -103.27^0 V_{se_2} = 0.240, θ_{se_2} = -94.84^0	V_{se_1} = 0.1383, θ_{se_1} = -107.53^0 V_{se_2} = 0.1176, θ_{se_2} = -82.19^0
I_{se_1} = 2.327, I_{se_2} =2.075 (p.u)	I_{se_1} = 3.60, I_{se_2} = 3.530 (p.u)
P_{ex_1} = 2.642, P_{ex_2} = -2.642 (MW)	P_{ex_1} =14.64, P_{ex_2} = -14.64(MW)

$Q^{sp}_{167-130} = -12.0$ MVAr, and $P^{sp}_{168-130} = -200.0$ MW.

Case 7) It is similar to case 6, except that IPFC is operating with the setpoint $P^{sp}_{167-130} = -350.0$ MW, $Q^{sp}_{167-130} = -80.0$ MVAr, and $P^{sp}_{168-130} = -350.0$ MW.

The solutions of cases 6 and 7 are listed in Table V.

In the following, six cases based on cases 6 and 7 are carried out to illustrate the constraints enforcement of IPFC. In order to obtain the violation states, the limits of IPFC are set to comparatively smaller values.

Case 8) It is similar to case 6, except that $V^{\max}_{se_2} = 0.24$ p.u.
Case 9) It is similar to case 7, except that $I^{\max}_{se_1} = 3.6$ p.u.
Case 10) It is similar to case 7, except that $P^{\max}_{ex_1} = 6.5$ MW.
Case 11) It is similar to case 10, except that $V^{\max}_{se_2} = 0.11$ p.u.
Case 12) It is similar to case 9, except that $V^{\max}_{se_1} = 0.13$ p.u.
Case 13) It is similar to case 12, except that $P^{\max}_{ex_1} = 14.0$ MW.

The solutions of cases 8–13 are listed in Tables VI–VIII in sequence. How the constraints enforcement of IPFC affects the number of iterations for converged cases is listed in Table IX.

From Tables V–VIII, IPFC has the capability to balance both active and reactive power flow between the lines because of the common dc link, transfer active power from overloaded to underloaded line, compensate against reactive voltage drops and the corresponding line reactive power, and thereby optimize the utilization of the over transmission system. It can be seen that when one or more of the constraints of IPFC are violated, the model ignores the original control objective and modifies power flow control toward the satisfactory control parameters within

TABLE VII
IPFC POWER FLOW SOLUTIONS FOR CASES 10 AND 11

Case 10	Case 11
V_{130}= 1.011, V_{167} = 0.987 V_{168}=0.996	V_{130}= 1.011, V_{167} = 0.987 V_{168}=0.996
$P_{167-130}$ = -350.0, $Q_{130,167}$ = -79.03 $P_{168-130}$ = -350.0, $Q_{168,130}$ = 24.56	$P_{167-130}$ = -350.0, $Q_{167-130}$ = -79.38 $P_{168-130}$ = -352.9, $Q_{168-130}$ = 24.47
V_{se_1} = 0.1337, θ_{se_1} = -95.50^0 V_{se_2} = 0.1116, θ_{se_2} = -94.71^0	V_{se_1} = 0.1326, θ_{se_1} = -95.43^0 V_{se_2} = 0.110, θ_{se_2} = -94.73^0
I_{se_1} = 3.623, I_{se_2} = 3.530 (p.u)	I_{se_1} =3.622, I_{se_2} = 3.557 (p.u)
P_{ex_1} = -6.50, P_{ex_2} = 6.50 (MW)	P_{ex_1} = -6.50, P_{ex_2} = 6.50 (MW)

TABLE VIII
IPFC POWER FLOW SOLUTIONS FOR CASES 12 AND 13

Case 12	Case 13
V_{130}= 1.009, V_{167} = 0.960 V_{168}=1.013	V_{130}= 1.009, V_{167} = 0.960 V_{168}=1.013
$P_{167-130}$ = -345.7, $Q_{130,167}$ = -1.84 $P_{168-130}$ = -350.0, $Q_{168,130}$ = -79.9	$P_{167-130}$ = 345.7, $Q_{167-130}$ = -2.36 $P_{168-130}$ = -350.0, $Q_{168-130}$ = -79.2
V_{se_1} = 0.130, θ_{se_1} = -107.26^0 V_{se_2} = 0.1174, θ_{se_2} = -82.46^0	V_{se_1} = 0.13, θ_{se_1} = -107.19^0 V_{se_2} = 0.1173, θ_{se_2} = -82.53^0
I_{se_1} = 3.6, I_{se_2} = 3.530 (p.u)	I_{se_1} = 3.6, I_{se_2} = 3.53 (p.u)
P_{ex_1} =14.13, P_{ex_2} = -14.13 (MW)	P_{ex_1} =14.0, P_{ex_2} = -14.0 (MW)

TABLE IX
EFFECT OF THE CONSTRAINTS ENFORCEMENT ON IPFC POWER FLOW CONVERGENCE

Case	Number of iterations	Case	Number of iterations
6	8	10	8
7	7	11	10
8	10	12	13
9	11	13	15

their limits. From Table IX, the constraints enforcement requires more iterations for converged solutions. Generally, one or two iterations are added when a limit is violated. Especially for the master line, if reducing the specified reactive power flow to zero cannot eliminate the series current limit violation, more iterations may be required.

V. CONCLUSION

A novel power injection model of IPFC suitable for power flow is presented. In this model, the impedance of the series converter coupling transformer and the line charging susceptance are all included, while the original structure and symmetry of admittance matrix can still be kept. Furthermore, the model can take into account the practical constraints of IPFC. Numerical results based on the IEEE 57-bus and IEEE 300-bus systems have shown the convergence and efficiency of the IPFC model. The power flow control capability and the constraints enforcement of IPFC are also exhibited.

Newton power flow program with this IPFC model is a useful tool for power system planning and operation control of large scale power system. The multiline control capability

of the IPFC will be likely to play an important role in solving many of the potential problems such as transmission network congestion management that transmission companies are now facing in the deregulated electricity market environment.

REFERENCES

[1] K. K. Sen, "SSSC-static synchronous series compensator theory, modeling, and application," *IEEE Trans. Power Del.*, vol. 13, no. 1, pp. 241–246, Jan. 1998.

[2] ——, "STATCOM-static synchronous compensator theory, modeling, and applications," in *Proc. IEEE Power Eng. Soc. Winter Meeting*, 1999, vol. 2, pp. 1177–1183.

[3] C. Schauder, M. Gernhardt, E. Stacey, T. Lemak, L. Gyugyi, T. W. Cease, and A. Edris, "TVA STATCOM project: design, installation, and commissioning," presented at the CIGRE Meeting, Paris, France, Aug. 1996, Paper 14-106, unpublished.

[4] K. K. Sen, "UPFC-unified power flow controller theory-modeling and applications," *IEEE Trans. Power Del.*, vol. 13, no. 4, pp. 1453–1460, Oct. 1998.

[5] C. D. Schauder, M. R. Lund, D. M. Hamai, T. R. Rietman, D. R. Torgerson, and A. Edris, "Operation of the unified power flow controller (UPFC) under practical constraints," *IEEE Trans. Power Del.*, vol. 13, no. 2, pp. 630–637, Apr. 1998.

[6] B. A. Renz, A. Keri, A. S. Mehraban, C. Schauder, E. Stacey, L. Kovalsky, L. Gyugyi, and A. Edris, "AEP unified power flow controller performance," *IEEE Trans. Power Del.*, vol. 14, no. 4, pp. 1374–1381, Oct. 1999.

[7] L. Gyugyi, K. K. Sen, and C. D. Schauder, "The interline power flow controller concept a new approach to power flow management in transmission systems," *IEEE Trans. Power Del.*, vol. 14, no. 3, pp. 1115–1123, Jul. 1999.

[8] S. Zelingher, B. Fardanesh, B. Shperling, S. Dave, L. Kovalsky, C. Schauder, and A. Edris, "Convertible static compensator project—hardware overview," in *Proc. IEEE Winter Meeting*, 2000, pp. 2511–2517.

[9] S. Arabi, H. Hamadanizadeh, and B. Fardanesh, "Convertible static compensator performance studies on the NY state transmission system," *IEEE Trans. Power Syst.*, vol. 17, no. 3, pp. 701–706, Aug. 2002.

[10] A. Nabavi-Niaki and M. R. Iravani, "Steady-state and dynamic models of unified power flow controller (UPFC) for power system studies," *IEEE Trans. Power Syst.*, vol. 11, no. 4, pp. 1937–1943, Nov. 1996.

[11] D. J. Gotham and G. T. Heydt, "Power flow control and power flow studies for systems with FACTS devices," *IEEE Trans. Power Syst.*, vol. 13, no. 1, pp. 60–65, Feb. 1998.

[12] H. Ambriz-Perez, E. Acha, C. R. Fuerte-Esquivel, and A. De la Torre, "Incorporation of a UPFC model in an optimal power flow using Newton's method," *Proc. Inst. Elect. Eng., Gen., Transm., Distrib.*, vol. 145, no. 3, pp. 336–344, May 1998.

[13] C. R. Fuerte-Esquivel, E. Acha, and H. Ambriz-Perez, "A comprehensive Newton-Raphson UPFC model for the quadratic power flow solution of practical power networks," *IEEE Trans. Power Syst.*, vol. 15, no. 1, pp. 102–109, Feb. 2000.

[14] M. Ghandhari, G. Anderson, and I. A. Hiskens, "Control Lyapunov functions or controllable series devices," *IEEE Trans. Power Syst.*, vol. 16, no. 4, pp. 689–693, Nov. 2001.

[15] M. Noroozian, L. Ängquist, M. Ghandhari, and G. Andersson, "Use of UPFC for optimal power flow control," *IEEE Trans. Power Del.*, vol. 12, no. 4, pp. 1629–1634, Oct. 1997.

[16] Y. Xiao, Y. H. Song, and Y. Z. Sun, "Power flow control approach to power systems with embedded FACTS devices," *IEEE Trans. Power Syst.*, vol. 17, no. 4, pp. 943–950, Nov. 2002.

[17] J. Y. Liu, Y. H. Song, and P. A. Mehta, "Strategies for handling UPFC constraints in steady-state power flow and voltage control," *IEEE Trans. Power Syst.*, vol. 15, no. 2, pp. 566–571, May 2000.

[18] X. P. Zhang, "Modeling of the interline power flow controller and the generalized unified power flow controller in Newton power flow," *Proc. Inst. Elect. Eng., Gen., Transm., Distrib.*, vol. 150, no. 3, pp. 268–274, May 2003.

[19] X. Wei, J. H. Chow, B. Fardanes, and A. Edris, "A common modeling framework of voltage-sourced converters for power flow, sensitivity, and dispatch analysis," *IEEE Trans. Power Syst.*, vol. 19, no. 2, pp. 934–941, May 2004.

[20] X. P. Zhang, "Advanced modeling of the multicontrol functional static synchronous series compensator (SSSC) in Newton power flow," *IEEE Trans. Power Syst.*, vol. 18, no. 4, pp. 1410–1416, Nov. 2003.

[21] J. Bian, D. G. Ramey, R. J. Nelson, and A. Edris, "A study of equipment sizes and constraints for a unified power flow controller," *IEEE Trans. Power Del.*, vol. 12, no. 3, pp. 1385–1391, Jul. 1997.

[22] S. Bruno and M. L. Scala, "Unified power flow controllers for security-constrained transmission management," *IEEE Trans. Power Syst.*, vol. 19, no. 1, pp. 418–426, Feb. 2004.

[23] Power Systems Test Case Archive Univ.Washington. Seattle. [Online]. Available: http://www.ee.washington.edu/research/pstca/.

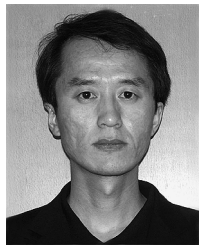

Yankui Zhang was born in China in 1973. He received the B.Sc. and M.Sc. degrees in electric engineering from China University of Mining and Technology, Beijing, China, in 1995 and 1998, respectively. He is currently pursuing the Ph.D. degree in the Department of Electrical Engineering, Shanghai Jiao Tong University, Shanghai, China.

He was with the electric power company of Henan province from 1998 to 2002. His research interests include FACTS technology, voltage stability, and electricity market operation.

Yan Zhang was born in China in 1958. She received the B.Sc. degree from Hefei University of Technology, Anhui, China, in 1982, the M.Sc. degree from China Electric Power Research Institute, Beijing, China, in 1987, and the Ph.D. degree from Shanghai Jiao Tong University, Shanghai, China, in 1998.

Currently, she is a Professor and Head of the School of Electronic, Information, and Electrical Engineering at Shanghai Jiao Tong University. Her research interests include power system planning, reliability, and distribution system automation

Chen Chen (SM'96) was born in Shanghai, China, in 1938. She received the graduation degree from Tsinghua University, Beijing, China, in 1964 and the Ph.D. degree in electric engineering from Purdue University West Lafayette, IN, in 1984.

She is currently a Professor of electrical engineering at Shanghai Jiao Tong University. Her research interests include power system stability and control and FACTS technology.